  Bull. Chem. Soc. Jpn., 56, 3434—3440 (1983) [Vol. 56, No. 11

Preparation and Spectroscopic Characterization of Substituted Pentacyanoferrates(II) with Phosphine or Phosphite Ligands

Hidenari Inoue,* Masahiro Sasagawa, Ekkehard Fluck,† and Tsuneo Shirai
Department of Applied Chemistry, Faculty of Science and Technology, Keio University, 3-14-1, Hiyoshi, Kohoku-ku, Yokohama 223
†*Institut für Anorganische Chemie, Universität Stuttgart, Pfaffenwaldring 55, D-7000 Stuttgart 80, FRG*
(Received May 6, 1983)

Twenty-two substituted pentacyanoferrates(II) with the formula $Na_3[Fe(CN)_5PX_3]\cdot 2H_2O$ (PX_3 = phosphine or phosphite) have been prepared by ligand substitution of sodium amminepentacyanoferrate(II). The phosphite complexes show smaller isomer shifts than the phosphine complexes. The phosphine complexes involving an aryl or bulky phosphine exhibit larger quadrupole splitting than the phosphite complexes. These tendencies in Mössbauer parameters are discussed in terms of the π-acceptor capability of the phosphine and phosphite ligands. The linear dependence of the isomer shifts on both CN stretching frequencies and d-d transition energies is interpreted on the basis of the predominance of iron-to-phosphorus π back-donation.

Substantial interest continues in substituted pentacyanoferrates(II) prepared from hexacyanoferrates(II) by replacing one of the six cyanide ligands with a ligand having a nitrogen donor atom. In recent years a wide variety of substituted pentacyanoferrates(II) have been synthesized and extensively studied by Mössbauer,[1-3] ^{13}C NMR,[4-6] and X-ray photoelectron spectroscopy.[7-8] The focus of these spectroscopic studies is the Fe–N bond between the central iron(II) ion and the nitrogen-containing ligand. Substituted pentacyanoferrates(II) in which the sixth ligand is a phosphine or phosphite have received relatively little attention although they provide an excellent opportunity for investigating the Fe–P bond by spectroscopic methods. Spectroscopic investigations on these phosphine and phosphite complexes have been limited almost wholly to a few complexes having the phosphine as the sixth ligand of octahedral coordination.[9-10]

We have prepared a series of substituted pentacyanoferrates(II) of the type $Na_3[Fe(CN)_5PX_3]\cdot 2H_2O$, where PX_3 is a phosphine or phosphite ligands. The functional groups adjacent to the phosphorus ligand atom was varied systematically in order to understand the Fe–P bond on the basis of the σ-donor and π-acceptor properties of the phosphine and phosphite ligands. Another purpose of the present work is to learn how the functional groups attached to the donor phosphorus atom affect the electronic structure of the $[Fe(CN)_5PX_3]^{3-}$ moiety and how the coordination of the phosphine or phosphite ligand influences the Fe–C bonding between the iron(II) ion and the cyanide ligands.

Experimental

Materials. Sodium amminepentacyanoferrate(II) was prepared by a method in the literature.[11] Phosphine and phosphite ligands were purchased from Strem Chemicals Inc. and used without further purification. All solvents used were analytical reagent grade, except that the methanol used for measurement of the electronic spectra was spectrophotometric solvent grade obtained from Kanto Chemical Co., Inc.

Preparation of Compounds. Manupulations involving air-sensitive materials were performed in a nitrogen-filled glovebox. General aspects of the experimental techniques are similar to those described in the literature.[12] Typical procedures are described in detail here only for $Na_3[Fe(CN)_5P(CH_3)_3]\cdot 2H_2O$ and $Na_3[Fe(CN)_5P(OCH_3)_3]\cdot 2H_2O$. To a suspension of 1.0 g (3.1 mmol) of $Na_3[Fe(CN)_5NH_3]\cdot 3H_2O$ in 25 ml of methanol was added 0.28 g (3.7 mmol) of $P(CH_3)_3$. The reaction slurry was vigorously stirred in the dark at room temperature for 24 h. Filtration of the resultant heterogeneous reaction mixture afforded a yellow solution. Careful addition of 150 ml of diethyl ether to the filtrate caused a yellow solid to precipitate. This was filtered, recrystallized from methanol, and dried over silica gel. To a vigorously stirred suspension of 1.0 g (3.1 mmol) of $Na_3[Fe(CN)_5NH_3]\cdot 3H_2O$ in 25 ml of methanol was added 0.80 g (6.4 mmol) of $P(OCH_3)_3$. After stirring of the reaction slurry in the dark at room temperature for 24 h, the resulting yellow reaction mixture was filtered off. Diethyl ether (200 ml) was added to the filtrate to precipitate a pale yellow solid, which was filtered with a glass filter, recrystallized from methanol, and dried over silica gel. The compounds were identified by elemental analysis (C, H, and N), phosphorus spectrophotometry, and iron atomic absorption spectrophotometry.

Physical Measurements. Mössbauer spectra were obtained with a ^{57}Co source in palladium (The Radiochemical Centre, Amersham, England) using a Wissel constant-acceleration transducer coupled with a Canberra OMEGA-1 multichannel analyzer operated in time mode. The spectra obtained at 77 and 293 K were fitted to Lorentzian curves with an iterative least-squares computer program. The isomer shifts were referred to the symmetry center of six absorption lines of natural iron foil at 293 K. Infrared spectra were recorded with a Hitachi Perkin-Elmer Model 225 grating infrared spectrophotometer in the range 200 to 4000 cm^{-1} and with a JASCO A-3 infrared spectrophotometer in the range 330 to 5000 cm^{-1} using Nujol mulls and KBr pellets. Electronic spectra of the substituted pentacyanoferrates(II) in methanol solution were recorded on a JASCO UVIDEC-1 digital double-beam spectrophotometer in the range 200 to 800 nm using 1-cm quartz cells.

Results and Discussion

Preparation of Complexes. All the compounds were obtained as pale yellow, pale blue, or colorless fine crystalline powders. Two of twenty-two substituted pentacyanoferrates(II) were not obtained in a pure form. Among the phosphine ligands tris(4-di-

TABLE 1. ANALYTICAL DATA OF $Na_3[Fe(CN)_5PX_3]\cdot 2H_2O$

No.	Ligand PX_3	Found (Calcd)(%)				
		C	H	N	Fe	P
1	$P[C_6H_4N(CH_3)_2]_3$	35.16 (51.04)	4.37 (5.02)	16.64 (16.42)	12.30 (8.18)	2.64 (4.54)
2	$P[CH(CH_3)_2]_3$	36.25 (37.27)	5.06 (5.58)	15.02 (15.52)	9.43 (12.38)	6.56 (6.87)
3	$P(C_6H_4F)_3$	40.01 (45.50)	2.63 (2.66)	10.38 (11.53)	7.74 (9.20)	4.36 (5.10)
4	$P(C_6H_4Cl)_3$	39.01 (42.08)	2.94 (2.46)	10.19 (10.67)	7.69 (8.51)	4.10 (4.72)
5	$P(C_6H_5)H_2$	32.24 (32.95)	2.49 (2.76)	15.97 (17.46)	14.51 (13.93)	7.39 (7.72)
6	$P(C_6H_4CH_3\text{-}m)_3$	48.52 (52.46)	4.26 (4.23)	11.39 (11.76)	10.19 (9.38)	5.00 (5.20)
7	$P(C_6H_4CH_3\text{-}p)_3$	48.90 (52.46)	4.33 (4.23)	11.43 (11.76)	9.14 (9.38)	4.56 (5.20)
8	$P(C_4H_9)_3$	38.31 (41.40)	5.65 (6.33)	13.33 (14.20)	11.34 (11.32)	5.94 (6.28)
9	$P(C_6H_5)_2H$	45.04 (42.80)	3.59 (3.17)	14.12 (14.68)	10.53 (11.70)	6.40 (6.49)
10	$P(C_6H_5)_3$	46.76 (49.93)	3.81 (3.46)	11.88 (12.66)	10.80 (10.09)	5.57 (5.60)
11	$P(C_2H_5)_3$	30.01 (32.30)	4.15 (4.68)	15.03 (17.12)	12.04 (13.65)	7.63 (7.57)
12	$P(C_6H_4OCH_3)_3$	40.54 (48.54)	3.78 (3.92)	10.09 (10.89)	9.23 (8.68)	4.19 (4.81)
13	$P(CH_3)_3$	25.86 (26.18)	3.36 (3.57)	18.58 (19.08)	12.75 (15.22)	5.38 (8.44)
14	$P[N(CH_3)_2]_3$	29.80 (29.09)	4.03 (4.88)	22.93 (24.67)	10.84 (12.30)	7.32 (6.82)
15	$P(C_6H_5)(OC_4H_9)_2$	41.94 (41.85)	4.91 (4.99)	13.22 (12.84)	11.62 (10.24)	4.95 (5.68)
16	$P(OC_4H_9)_3$	38.20 (37.72)	5.42 (5.77)	13.40 (12.94)	11.61 (10.32)	4.58 (5.72)
17	$P(OC_2H_5)_3$	29.10 (28.90)	3.87 (4.19)	15.55 (15.32)	12.59 (12.22)	5.95 (6.78)
18	$P(C_6H_5)_2(OC_4H_9)$	42.11 (45.92)	3.87 (4.22)	11.70 (12.75)	9.20 (10.19)	4.96 (5.64)
19	$P(OCH_2CH_2Cl)_3$	22.55 (23.58)	3.28 (2.88)	11.31 (12.50)	9.67 (9.97)	6.05 (5.53)
20	$P(OCH_3)_3$	23.20 (23.15)	3.04 (3.16)	17.04 (16.88)	12.96 (13.46)	7.19 (7.46)
21	$P[OCH(CH_3)_2]_3$	34.01 (33.69)	4.67 (5.05)	14.22 (14.03)	11.37 (11.19)	5.81 (6.21)
22	$P(OC_6H_5)_3$	43.61 (45.95)	3.78 (3.19)	14.53 (11.65)	10.41 (9.29)	5.25 (5.15)

methylaminophenyl)phosphine failed to give pure $Na_3[Fe(CN)_5P(C_6H_4N(CH_3)_2)_3]\cdot 2H_2O$ because the ligand is only slightly soluble in methanol. A mixture of methanol and acetone (1:1) was used to improve the solubility of the ligand and the reaction product. However, the Mössbauer spectra of the products always gave a couple of quadrupole-splitting doublets, indicating that the desired product was contaminated. Among the phosphite ligands triphenyl phosphite appeared to undergo ester interchange with the solvent, *i.e.*, with methanol to yield four different types of phosphite complexes with mixed phosphites such as $P(OC_6H_5)_3$, $P(OC_6H_5)_2(OCH_3)$, $P(OC_6H_5)(OCH_3)_2$, and $P(OCH_3)_3$. The existence of these four pentacyanophosphiteferrate(II) species was confirmed by ^{31}P NMR spectroscopy because each coordinated phosphite ligand shows a characteristic chemical shift. When *N,N*-dimethylformamide was used in place of methanol as the solvent, the desired complex was contaminated by sodium pentacyano(*N,N*-dimethylformamide)ferrate(II). This contamination was confirmed by a comparison of Mössbauer parameters.

Effect of Axial Ligand on Isomer Shift. The series of complexes prepared here are suitable model compounds for studying the Fe–P bond without changing the type of coordination bonding, *i.e.*, the atomic orbital which participate in the Fe–P bond. Especially Mössbauer spectroscopy provides a sophisticated means to characterize the Fe–P bond in the present complexes. Typical Mössbauer spectra obtained are presented in Fig. 1. Most of our complexes gave a symmetric quadrupole-splitting doublet although the

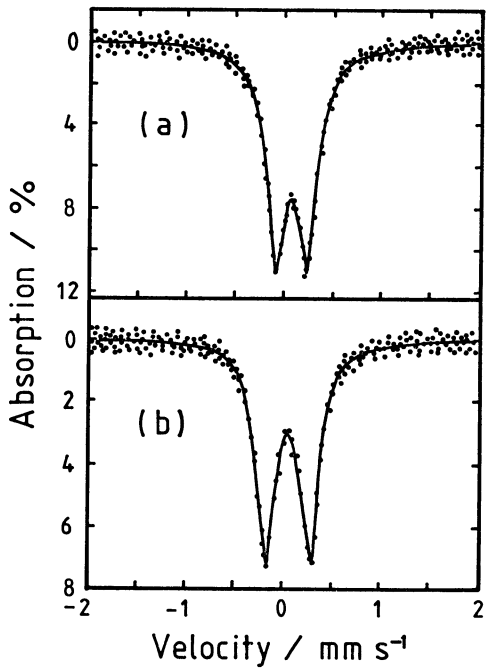

Fig. Typical Mössbauer spectra of (a) $Na_3[Fe(CN)_5P(CH_3)_3]\cdot 2H_2O$ and (b) $Na_3[Fe(CN)_5P(OC_2H_5)_3]\cdot 2H_2O$ at 77 K.

complexes having diphenylphosphine or phenylphosphine ligand showed an asymmetric doublet even at 77 K. In these complexes the higher velocity component of the quadrupole-splitting doublet was always stronger than the lower one, and this asymmetry remained even in measurements with finely ground powders. The Mössbauer parameters are summarized in Table 2. The isomer shifts at 77 K are more positive than those at 293 K due to the second-order Doppler shift. The isomer shifts obtained at 293 K range from −0.075 to 0.012 mm/s and fall into the range characteristic of low-spin iron(II) complexes.

In general the isomer shift in iron compounds increases with a decrease in total electron density at the iron nucleus.[13] Electrons other than s electrons do not contribute directly to the total electron density at the iron nucleus, *i.e.*, to the isomer shift, because of a negligibly small probability density at the nucleus. However, d electrons affect the total electron density at the iron nucleus through the so-called shielding effect. The change in the isomer shift is interpreted mainly by the following two mechanisms; ligand-to-metal σ donation and metal-to-ligand π back-donation. Both mechanisms increase the total electron density at the iron nucleus, and hence decrease the isomer shift of iron complexes. The decreasing tendency of isomer shifts is clearly associated with the σ-donor and π-acceptor capability of the ligand PX_3, *i.e.*, the electronic properties of functional group X attached to the phosphorus atom. An increased σ-donor capability of the phosphorus ligand increases the s-electron density at the iron nucleus through the formation of the phosphorus-to-iron σ bonding. Increased π-acceptor capability of the phosphorus ligand also increases the s-electron density at the nucleus through π back-donation from the iron d_π orbital to the vacant

Table 2. Mössbauer parameters of $Na_3[Fe(CN)_5PX_3]\cdot 2H_2O$[a]

No.	Ligand PX_3	Isomer shift/mm s^{-1}		Quadrupole splitting/mm s^{-1}	
		293 K	77 K	293 K	77 K
1	$P[C_6H_4N(CH_3)_2]_3$	0.01_2	0.07_6	0.72_5	0.71_6
2	$P[CH(CH_3)_2]_3$	-0.02_4	0.05_0	0.47_8	0.48_7
3	$P(C_6H_4F)_3$	-0.03_1	0.03_3	0.69_4	0.67_8
4	$P(C_6H_4Cl)_3$	-0.03_7	0.03_0	0.64_3	0.62_8
5	$P(C_7H_5)H_2$	-0.03_7	0.04_3	0.50_0	0.48_6
6	$P(C_6H_4CH_3\text{-}m)_3$	-0.03_8	0.03_8	0.68_6	0.58_5
7	$P(C_6H_4CH_3\text{-}p)_3$	-0.04_0	0.02_9	0.64_4	0.62_5
8	$P(C_4H_9)_3$	-0.04_1	0.00_6	0.28_7	0.24_9
9	$P(C_6H_5)_2H$	-0.04_2	0.04_0	0.48_9	0.58_9
10	$P(C_6H_5)_3$	-0.04_4	0.03_1	0.64_8	0.63_3
11	$P(C_2H_5)_3$	-0.04_6	0.00_0	0.25_0	0.30_2
12	$P(C_6H_4OCH_3)_3$	-0.04_9	0.03_0	0.65_4	0.61_6
13	$P(CH_3)_3$	-0.05_7	0.01_4	0.32_0	0.30_6
14	$P[N(CH_3)_2]_3$	-0.05_8	0.00_1	0.41_5	0.41_9
15	$P(C_6H_5)(OC_4H_9)_2$	-0.05_9	0.01_4	0.46_5	0.48_9
16	$P(OC_4H_9)_3$	-0.06_0	0.00_4	0.41_0	0.39_4
17	$P(OC_2H_5)_3$	-0.06_0	0.00_8	0.44_9	0.44_1
18	$P(C_6H_5)_2(OC_4H_9)$	-0.06_3	0.02_9	0.48_4	0.51_4
19	$P(OCH_2CH_2Cl)_3$	-0.06_8	-0.00_5	0.38_6	0.40_6
20	$P(OCH_3)_3$	-0.06_9	-0.00_4	0.47_4	0.48_1
21	$P[OCH(CH_3)_2]_3$	-0.07_5	0.00_8	0.44_9	0.43_9
22	$P(OC_6H_5)_3$	-0.07_6	0.00_5	0.49_7	0.48_6

a) With uncertainty of 0.005 mm/s.

phosphorus π or d_π orbitals. Therefore, the σ-donor capability can not be readily differentiated from the π-acceptor capability by the isomer shift value, which reflects only the total electron density at the iron nucleus.

The isomer shifts of phosphite complexes are smaller than those of phosphine complexes. This indicates that the higher the electronegativity of the atom adjacent to the phosphorus atom the larger the isomer shift of the complexes. The electron-attracting and electron-releasing power of the substituent at the 4 position of the triarylphosphines is associated with the Hammett substituent constant, which decreases in the order $-Cl>-F>-H>-CH_3>-OCH_3>-N(CH_3)_2$.[14] This order was expected to be directly connected with the isomer shifts observed for $Na_3[Fe(CN)_5PX_3]\cdot 2H_2O$, where PX_3 is an arylphosphine with a substituent at the 4 position. However, no significant linear correlation could be established between the isomer shift and the Hammett substituent constant. Thus the substituent X on the aryl group is located too far away to affect the electron density at the iron nucleus, *i.e.*, the isomer shift of the central iron atom *via* the mesomeric or inductive effect.

The isomer shift of the complexes involving a phenylphosphine increases clearly in the sequence: $P(C_6H_5)_3<P(C_6H_5)_2H<P(C_6H_5)H_2$. The substitution of a phenyl group for a hydrogen diminishes the π-acceptor capability of the phosphorus donor atom and decreases the iron-to-phosphorus π back-donation. Consequently, this decrease in the back donation agrees

with the increased isomer shift observed for the complex having the phenylphosphine.

Influence of Local Symmetry on Quadrupole Splitting. The symmetry group of the $[Fe(CN)_5PX_3]^{3-}$ moiety is approximated as C_{4v} if the geometry of the three functional groups directly attached to the phosphorus atom is ignored. In $Na_3[Fe(CN)_5PX_3]\cdot 2H_2O$ the symmetry around the iron nucleus is distorted from the O_h symmetry to which the $Fe(CN)_6^{4-}$ moiety of sodium hexacyanoferrate(II) belongs. The local site symmetry of the $[Fe(CN)_5PX_3]^{3-}$ moiety is reflected in the quadrupole splitting of the Mössbauer spectra. All the complexes of the type $Na_3[Fe(CN)_5PX_3]\cdot 2H_2O$ show quadrupole splitting, whereas the octahedrally symmetric sodium hexacyanoferrate(II) shows no quadrupole splitting at all.[15] The quadrupole splittings of $Na_3[Fe(CN)_5PX_3]\cdot 2H_2O$ are relatively small and typical of low-spin iron(II) complexes. They increase slightly on lowering the temperature to 77 K since the low-spin iron(II) complex usually has only a small valence contribution to the electric field gradient at the iron nucleus. The arylphosphine complex gives a larger quadrupole splitting than does the alkylphosphine complex. This is presumably due to the bulkiness of the aryl groups. The quadrupole splitting values of the phosphite complex, as well as the complex with a ligand intermediate between phosphine and phosphite, lie between those of arylphosphine and alkylphosphine complexes.

The quadrupole splitting is plotted against the isomer shift in Fig. 2. A linear plot was obtained (r=0.702) for the measurements at 77 K.[16] Good correlation was not found (r=0.505) for the measurements at 293 K, probably due to the pronounced contribution of the second-order Doppler effect to the isomer shift. The isomer shift data alone do not always reveal which is dominant, the σ-donation or the π back-donation, because both increase the electron density at the iron nucleus and consequently decrease the isomer shift. Despite their similar contribution to the isomer shift the linear dependence of the quadrupole splitting on the isomer shift provides a useful means of estimating

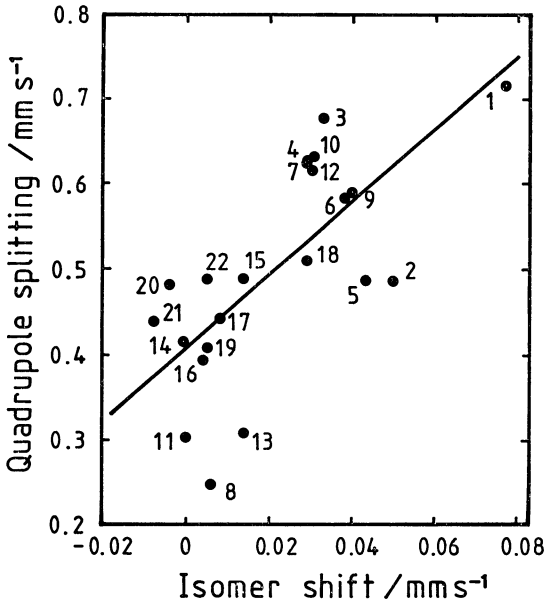

Fig. 2. Plots of quadrupole splittings against isomer shifts (at 77 K).

Table 3. Infrared frequencies observed for $Na_3[Fe(CN)_5PX_3]\cdot 2H_2O$

No.	Ligand PX_3	Absorption frequencies/cm^{-1}				
		$\nu_{CN}(1)$	$\nu_{CN}(2)$	$\nu_{CN}(3)$	δ_{Fe-CN}	ν_{Fe-C}
1	$P[C_6H_4N(CH_3)_2]_2$	2084^m	—	2039^s	578^m	vb
2	$P[CH(CH_3)_2]_3$	2088^m	2059^{sh}	2038^s	576^m	vb
3	$P(C_6H_4F)_3$	2086^m	—	2046^s	576^m	470^b
4	$P(C_6H_4Cl)_3$	2092^m	2070^{sh}	2045^s	578^m	434^b
5	$P(C_6H_5)H_2$	2090^m	—	2042^s	576^m	(500, 463)^b
6	$P(C_6H_4CH_3\text{-}m)_3$	2089^m	2067^{sh}	2042^s	579^m	468^b
7	$P(C_6H_4CH_3\text{-}p)_3$	2089^m	2066^{sh}	2041^s	578^m	436^b
8	$P(C_4H_9)_3$	2088^m	2060^{sh}	2043^s	586^m	(470, 440)^b
9	$P(C_6H_5)_2H$	2096^m	2075^{sh}	2052^s	578^m	472^b
10	$P(C_6H_5)_3$	2092^m	2072^{sh}	2057^s	577^m	460^b
11	$P(C_2H_5)_3$	2083^m	—	2038^s	580^m	vb
12	$P(C_6H_4OCH_3)_3$	2086^m	2062^{sh}	2042^s	578^m	(470, 432)^b
13	$P(CH_3)_3$	2088^m	—	2037^s	578^m	vb
14	$P[N(CH_3)_2]_3$	2092^m	—	2055^s	578^m	vb
15	$P(C_6H_5)(OC_4H_9)_2$	2100^m	2080^{sh}	2062^s	580^m	(438, 408)^b
16	$P(OC_4H_9)_3$	2094^m	2073^{sh}	2051^s	578^m	(450, 418)^b
17	$P(OC_2H_5)_3$	2100^m	2074^{sh}	2060^s	578^m	420^b
18	$P(C_6H_5)_2(OC_4H_9)$	2091^m	2068^{sh}	2048^s	578^m	vb
19	$P(OCH_2CH_2Cl)_3$	2100^m	2080^{sh}	2062^s	578^m	(447, 402)^b
20	$P(OCH_3)_3$	2092^m	2069^{sh}	2050^s	578^m	(443, 412)^b
21	$P[OCH(CH_3)_2]_3$	2097^m	2075^{sh}	2050^s	580^m	430^b
22	$P(OC_6H_5)_3$	2104^m	2088^{sh}	2062^s	577^m	(418, 400)^b

s, strong; m, medium; sh, shoulder; b, broad; vb, very broad.

the relative importance of the σ-donor or π-acceptor capability.[17] The linear dependence with a positive slope demonstrates that the σ-donation is offset by the π-acceptor, *i.e.*, the π-acceptor capability is dominant in the present complexes.

Dependence of IR Frequencies on π-Acceptor Capability of Ligand PX_3. The infrared frequencies are summarized in Table 3. The ν_{CN} stretching modes referred to as $\nu_{CN}(1)$, $\nu_{CN}(2)$, and $\nu_{CN}(3)$ in Table 3 appeared in the range 2030—2100 cm^{-1}. The observation of two or three ν_{CN} stretching bands is consistent with the group-theoretical prediction that the point group of the $[Fe(CN)_5PX_3]^{3-}$ moiety is approximately C_{4v}. The dependence of the ν_{CN} stretching frequencies on the isomer shift is useful for estimating the π-acceptor capability of the ligand PX_3. As shown in Fig. 3, all the frequencies observed for the $\nu_{CN}(1)$, $\nu_{CN}(2)$, and $\nu_{CN}(3)$ stretching modes decrease as the isomer shifts increase. This decrease in the ν_{CN} stretching frequencies reflects the reduced Fe-to-P π back-donation. The stronger the π-acceptor capability of the ligand PX_3 is the more the d_π electrons of the central iron atom are withdrawn towards the ligand through π back-donation. Alternatively, the decreased electron density in the iron d_π orbitals is compensated for by increased electron flow from the cyanide ligands to the central iron atom through the inverse π back-donation. Thus the decreased electron population in the antibonding π^* orbitals of the cyanide ligands causes the ν_{CN} stretching frequencies to increase. The relative increase in the Fe-to-P back-donation gives rise to the increased total electron density at the iron nucleus because of the decreased shielding effect of its d_π electrons and hence leads to the decreased isomer shift. This indicates that the greatly increased π back-donation from the filled iron d_π orbitals to the phosphorus orbitals is not offset, even by the decreased π back-donation to the cyanide ligands. All the ν_{CN} stretching modes belonging to the two different species $2A_1+E$ showed the same tendency with regard to the dependence of the ν_{CN} stretching frequencies on the isomer shifts. The empty antibonding π^* orbitals of both axial and radial cyanide ligands participate in overlapping with the identical d_π orbitals to form the π bonding between Fe and C. Accordingly, the same tendency observed for three different ν_{CN} stretching modes is due to the synergetic effect of the d_π orbitals of the central iron atom on the axial and radial cyanide ligands.

The ν_{Fe-C} stretching and δ_{Fe-CN} bending modes appeared in the ranges 400—500 and 576—586 cm^{-1}, respectively. The ν_{Fe-C} stretching mode of the complexes with a phosphine ligand tends to show higher absorption frequencies than those with a phosphite ligand. This tendency agrees with the fact that the Fe-to-P back-donation is generally larger in phosphite complexes than in phosphine complexes. On the other hand, the absorption frequencies of the δ_{Fe-CN} bending modes were almost independent of the kind of phosphorus ligand. The ν_{Fe-P} stretching and δ_{Fe-P} bending modes are expected to be direct evidence for the Fe–P bonding. Unfortunately, no absorption band could be observed for our complexes, presumably because these absorption bands are of very weak intensity or lie outside of the present experimental region.

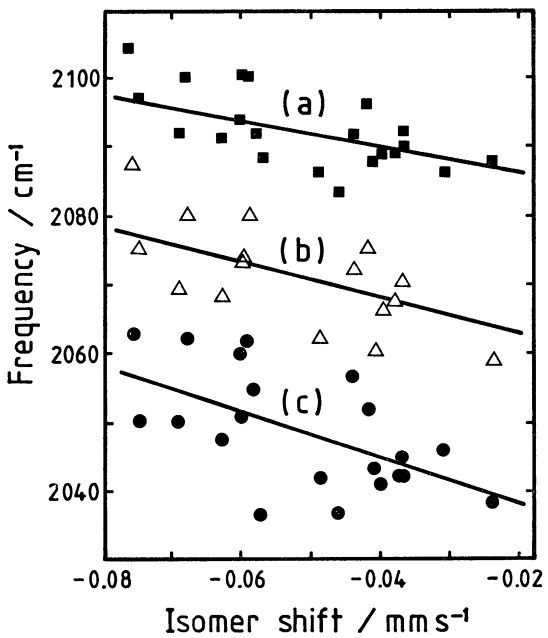

Fig. 3. Dependence of three different ν_{CN} stretching frequencies on isomer shifts. (a), (b), and (c) correspond to a regression line for the $\nu_{CN}(1)$, $\nu_{CN}(2)$, and $\nu_{CN}(3)$ stretching modes. Plots of compound No. 1 are not shown here due to its large positive isomer shift (at 293 K).

TABLE 4. ELECTRONIC SPECTRA OF $Na_3[Fe(CN)_5PX_3]\cdot 2H_2O$

No.	Ligand PX_3	Observed wave number/10^3 cm^{-1}		
		$^1A_1\rightarrow E(1)$	$^1A_1\rightarrow {}^1A_2$	$^1A_1\rightarrow E(2)$
1	$P[C_6H_4N(CH_3)_2]_3$	24.9^{sh}	vw	vw
2	$P[CH(CH_3)_2]_3$	29.5^{sh}	25.2^{sh}	17.7^{w}
3	$P(C_6H_4F)_3$	26.3^{sh}	vw	17.3^{w}
4	$P(C_6H_4Cl)_3$	vw	vw	vw
5	$P(C_6H_5)H_2$	29.2^{sh}	25.0^{sh}	vw
6	$P(C_6H_4CH_3\text{-}m)_3$	26.3^{sh}	vw	17.1^{w}
7	$P(C_6H_4CH_3\text{-}p)_3$	26.0^{sh}	vw	17.0^{w}
8	$P(C_4H_9)_3$	30.0^{sh}	25.0^{sh}	18.2^{w}
9	$P(C_6H_5)_2H$	27.2^{sh}	vw	16.8^{w}
10	$P(C_6H_5)_3$	26.5^{sh}	vw	18.0^{w}
11	$P(C_2H_5)_3$	30.3^{sh}	25.0^{sh}	18.2^{w}
12	$P(C_6H_4OCH_3)_3$	27.5^{sh}	24.5^{sh}	15.5^{w}
13	$P(CH_3)_3$	30.4^{sh}	25.1^{sh}	20.0^{w}
14	$P[N(CH_3)_2]_3$	30.8^{sh}	25.0^{sh}	vw
15	$P(C_6H_5)(OC_4H_9)_2$	29.5^{sh}	25.0^{sh}	vw
16	$P(OC_4H_9)_3$	31.3^{sh}	25.8^{sh}	20.0^{w}
17	$P(OC_2H_5)_3$	31.2^{sh}	25.0^{sh}	20.5^{w}
18	$P(C_6H_5)_2(OC_4H_9)$	31.0^{sh}	vw	vw
19	$P(OCH_2CH_2Cl)_3$	31.6^{sh}	25.0^{sh}	vw
20	$P(OCH_3)_3$	30.8^{sh}	vw	20.2^{w}
21	$P[OCH(CH_3)_2]_3$	30.8^{sh}	24.1^{sh}	20.0^{w}
22	$P(OC_6H_5)_3$	30.5^{sh}	24.5^{sh}	vw

sh: shoulder; w: weak; vw: very weak.

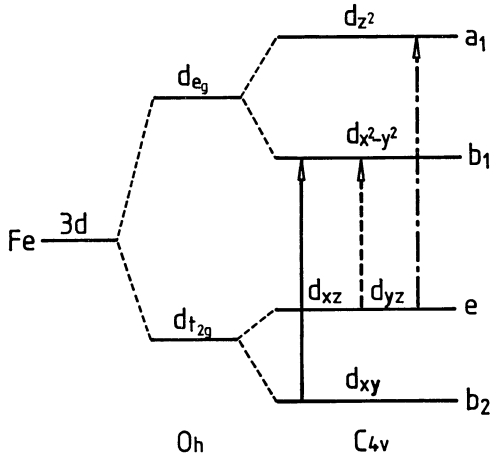

Fig. 4. Energy-term diagram for the $[Fe(CN)_5PX_3]^{3-}$ moiety. (a) $^1A_1 \rightarrow E(1)$ (—·—·—), (b) $^1A \rightarrow {}^1A_2$ (——), and (c) $^1A_1 \rightarrow E(2)$ (----).

Correlation between d-d Transition Energy and π Back-Donation. The absorption bands observed in the electronic spectra are presented in Table 4 together with their assignment. The electronic spectra of these complexes are so similar to those of the usual substituted pentacyanoferrates(II) that the absorption bands were assigned by comparison with the band assignment for substituted pentacyanoferrates(II) such as sodium pentacyanonitrosylferrate(II).[18] The partial energy-term diagram of the $[Fe(CN)_5PX_3]^{3-}$ moiety (symmetry group C_{4v}) is schematically shown in Fig. 4. A strong absorption band observed in the range 26×10^3—32×10^3 cm^{-1} is assigned to the transition $^1A_1 \rightarrow E(1)$ ($e \rightarrow a_1$). A relatively weak absorption band assigned to the transition $^1A_1 \rightarrow E(2)$ ($e \rightarrow b_1$) appeared in the range 15×10^3—21×10^3 cm^{-1}. A weak shoulder band around 25×10^3 cm^{-1} is assigned to the transition $^1A_1 \rightarrow {}^1A_2$ ($b_2 \rightarrow b_1$) although it is partially hidden by the strong absorption band resulting from the transition $^1A_1 \rightarrow E(1)$. The band position of the transition $^1A_1 \rightarrow {}^1A_2$ is hardly affected by the variation in the axial phosphine or phosphite ligand, while those of the other transitions, $^1A_1 \rightarrow E(1)$ and E(2), vary with the kind of axial ligand. This is due to the fact that both transitions $^1A_1 \rightarrow E(1)$ and E(2) involve the d_{xz} and d_{yz} orbitals directed towards the axial phosphine or phosphite ligand.

The transition energies of the d-d absorption bands are correlated with the isomer-shift values since both ligand field parameters and Mössbauer parameters are associated with the π-acceptor capability of the axial ligand.[19] The plots of the d-d transition energies *vs.* the isomer shift values are shown in Fig. 5. The energies of the transitions $^1A_1 \rightarrow E(1)$ and E(2) decrease as the isomer shifts increase, whereas the energy of the transition $^1A_1 \rightarrow {}^1A_2$ is almost independent of the variation in the isomer shifts as the axial phosphine or phosphite ligands are changed. This relationship between the d-d transition energies and the isomer shifts can be also explained on the basis of the Fe-to-P π back-donation. The energy level e (shown in Fig. 4) is lowered by the enhanced Fe-to-P π back-donation so that the energies of the transitions $^1A_1 \rightarrow E(1)$ and E(2) are increased and shifted to the higher frequency side.

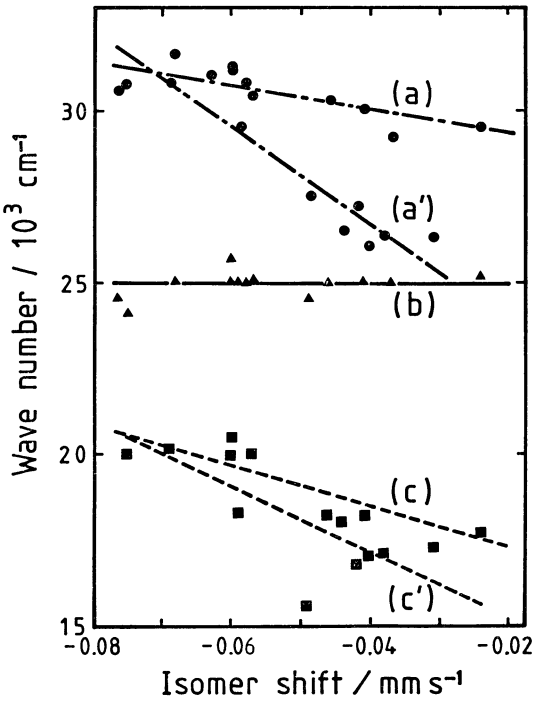

Fig. 5. Plots of d-d transition energies *vs.* isomer shifts (at 293 K). (a) and (c) are a regression line for alkylphosphine complexes, (a') and (c') for arylphosphine complexes, and (b) for both phosphine complexes. Plots of compound No. 1 are not shown here due to its large positive isomer shift.

References

1) P. J. Aymonino, M. A. Blesa, J. A. Olabe, and E. Frank, *Z. Naturforsch., B*, **31**, 1532 (1976).
2) C. P. Monaghan and J. C. Fanning, *J. Phys. Chem.*, **82**, 1045 (1978).
3) A. N. Garg and P. N. Shukla, *Z. Naturforsch., B*, **36**, 59 (1981).
4) B. A. Narayanan and P. T. Manoharan, *J. Inorg. Nucl. Chem.*, **40**, 1993 (1978).
5) H. Toma, J. A. Vanin, and J. M. Malin, *Inorg. Chim. Acta*, **33**, L157 (1979).
6) J. Jwo, P. L. Gaus, and A. Haim, *J. Am. Chem. Soc.*, **101**, 6189 (1979).
7) H. Binder, *Z. Anorg. Allg. Chem.*, **429**, 247 (1977).
8) K. B. Yatsimirskii, V. V. Nemoshkalenko, Yu. P. Nazarenko, V. G. Aleshin, V. V. Zhilinskaya, and A. Tomashevsky, *J. Electron Spectrosc. Relat. Phenom.*, **10**, 239 (1977).
9) E. Fluck and P. Kuhn, *Z. Anorg. Allg. Chem.*, **350**, 263 (1967).
10) K. Burger, L. Korecz, S. Papp, and B. Mohai, *Radiochem. Radioanal. Lett.*, **2**, 153 (1969).
11) D. J. Kenney, T. P. Flynn, and J. B. Gallini, *J. Inorg. Nucl. Chem.*, **20**, 75 (1961).
12) V. R. Nast and K. W. Krüger, *Z. Anorg. Allg. Chem.*, **341**, 189 (1965).
13) N. N. Greenwood and T. C. Gibb, "Mössbauer Spectroscopy," Chapman and Hall, London (1971), Chap. 5.

14) L. S. Hammett, "Physical Organic Chemistry," McGraw-Hill, New York (1970), Chap. 11.
15) H. Inoue, E. Fluck, H. Binder, and S. Yanagisawa, *Z. Anorg. Allg. Chem.*, **483**, 75 (1981).
16) The correlation coefficient r calculated from the measurements at 77 K is significant at the 0.005 significant level, while that obtained for the measurements at 293 K is significant at the 0.05 significant level.
17) B. A. Sosinsky, N. Norem, and R. G. Shong, *Inorg. Chem.*, **21**, 4229 (1982).
18) P. T. Manoharan and H. B. Gray, *J. Am. Chem. Soc.*, **87**, 3340 (1965).
19) H. E. Toma, E. Giesbrecht, J. M. Malin, and E. Fluck, *Inorg. Chim. Acta*, **14**, 11 (1975).